OPEN ACCESS

Kashf Journal of Multidisciplinary Research
Vol: 02 - Issue 06 (2025)
P-ISSN: 3007-1992 E-ISSN: 3007-200X
https://kjmr.com.pk

GREEN SYNTHESIS OF SILVER NANOPARTICLES USING STEM AERVA JAVANICA

[1] ***Ghulam Murtaza Khan****
Department of Chemistry, University of Science and Technology Bannu, Pakistan.
[2] ***Waqar Ahmad***
Department of Chemistry, University of Science and Technology Bannu, Pakistan.
[3] ***Mirza Nauman Ashraf***
Department of Chemistry, The Scholars Science College, The Mall Wah Cantt, Pakistan.
[4] ***Adeel Hussain Chughtai***
Institute of Chemical Sciences Bahauddin Zakariya University, Multan (60800), Pakistan.
[5] ***Abrar Hussain***
Graduate Institute of Biological Science & Technology, China Medical University, Taiwan.
[6] ***Abdul Qayyum***
Department of Chemistry, Government College University Lahore, Pakistan.
[7] ***Muhammad Abdul Salam***
Department of chemistry Khushal Khan khattak University Karak,Pakistan.
[8] ***Fatima Aziz***
Shifa College of Pharmaceutical Sciences (SCPS), Shifa Tameer-e-Millat University, Islamabad, Pakistan.

[*] ***Corresponding author: Ghulam Murtaza Khan*** (ghulammurtazakhan6196@gmail.com)

Article Info

Abstract

Aerva javanica, one of the well-established medicinally essential plants, was employed for biosynthesizing silver nanoparticles (AJ@AgNPs) using a green procedure using an aqueous stem extract. The plant material was dried in the shade and the AJ@AgNPs formation mediated by the extract was confirmed with UV-vis spectrophotometry, which exhibited an indicative surface plasmon resonance peak at 414 nm. The AJ@AgNPs showed selective colorimetric sensing for Cu2+ ions from yellow to light pink and had a linear detection range of 1–50 µM and practical application in tap water analysis. The nanoparticles (NPs) showed high antibacterial activity against Klebsiella pneumonia, Staphylococcus aureus, and Escherichia coli compared with the crude extract, and was possibly due to synergistic action between silver ions and phytochemicals. Synthesis conditions, such as pH and extract concentration, significantly affected AJ@AgNPs were investigated. These results demonstrate the dual potential of AJ@AgNPs as a sensitive environmental sensor and antimicrobial agent, with pH and extract optimization providing scalable approaches to biomedical and environmental applications.

Keywords:
AJ@AgNPs, colorimetric sensing, green synthesized, antibacterial activity, Cu2+ detection

Introduction

Working with materials on a nanolevel (1-100 nm), nanotechnology has had a significant impact on modern science[1]. Synthetic functional materials with improved physical, chemical, and biological characteristics are now possible because to this technology[2],[3]. Owing to their very large surface area relative to their volume and the quantum confinement effects, nanoparticles (NPs) have unique optical, catalytic, and electrical characteristics and so constitute the engine behind this revolution[4]. Because of these qualities, NPs have been great help in many other fields like environmental research, health, energy, and industry[5]. For each intended usage, researchers have looked at a variety of metal and metal oxide nanoparticles during the last decades: gold[6], iron oxide[7], titanium dioxide[8], zinc oxide[9], and silver.

Because of their amazing physicochemical properties and extensive uses, silver nanoparticles (AgNPs) are a cornerstone of nanotechnology among metal NPs[10]. Since ancient times, silver has been employed for its antibacterial properties; its nanoform improves the effects employing more reactivity and surface contact. AgNPs are appropriate for optical sensing, SERS, and photonic uses as they exhibit strong surface plasmon resonance in the visible spectrum, which shows as significant color shifts[11]. Conventional NPs synthesis via chemical or physical reduction, however, leaves behind ecologically stable residues and uses hazardous stabilizers[12]. These constraints have driven the need for methods that lower waste, are cost-effective, avoid the use of hazardous chemicals, and enhance biocompatibility. Green synthesized NPs solve this problem[13].

Using biological systems like plant extracts, algae, fungus, or bacteria, green synthesis—an ecologically benign method—reduces metal ions and caps NPs. Using plants is simple, scalable, and affordable[14]. Plant extracts include phytochemicals—flavonoids, polyphenols, terpenoids, and alkaloids—acting as natural reducing and capping agents unlike microbiological techniques, which need stringent aseptic conditions and extensive incubation times[15]. These biomolecules provide quick NP production and also provide functional coatings enhancing stability and bioactivity[16].

Here, an underutilized source for green synthesis is Aerva javanica, a drought-resistant plant from arid and semi-arid surroundings, which is used for synthesizing AgNPs[17]. Applied historically in traditional medicine for the treatment of kidney diseases, inflammation, and microbial infections, Aerva javanica contains bioactive molecules including alkaloids, saponins, and phenolics, which are postulated to have dual functions in NP synthesis: silver ion reduction (Ag^{+} to Ag^{0}) and stabilisation of the formed NPs[18]. Although past studies have examined the leaves and roots of Aerva javanica for medicinal uses, its stem—a structurally stiff and less-researched component—has promise as a sustainable nanomaterial building block[19]. Through the stem extract, this work not only gives value to agricultural waste but also investigates the combined impact of its unique phytochemical composition on the characteristics of AgNPs.

Apart from synthesis, AgNPs have shown considerable promise in addressing two of the most pressing worldwide issues: environmental pollution and antibiotic resistance[20]. The ecology and human health are seriously threatened by heavy metal contamination including copper ions (Cu^{2+})[21]. Although copper is a trace necessary metal, too much of it causes interference with cellular operations that leads to neurological illness, liver toxicity, and ecological damage[21]. Although inductively coupled plasma mass spectrometry (ICP-MS) and atomic absorption spectroscopy (AAS) are sensitive traditional detection methods for Cu^{2+}, they need complex apparatus, skilled staff, and labour-intensive sample preparation[22]. By comparison, colorimetric sensing based on NPs offers a portable, reasonably priced, quick solution[23]. Concurrent with this development of antibiotic-resistant bacteria, new antimicrobial agents are desperately needed[24]. AgNPs provide a powerful answer by means of their way of interfering with the cell membrane of bacteria, thus preventing enzymatic activity, and so generating reactive oxygen

species (ROS)[25]. Because the synergistic impact of silver and phytochemicals endogenous to the plant extract is involved, green-synthesized AgNPs might have better antibacterial efficacy[26]. Here we provide a green synthesis route for AgNPs from Aerva javanica stem extract with an eye towards their two uses as efficient antibacterial agents and selective colorimetric sensor for Cu^{2+} ions. This work advances the frontiers of ecologically friendly material synthesis by merging green chemistry ideas with nanotechnology, therefore fulfilling basic needs in environmental protection and medical. The originality here is the unrealised adaptability of Aerva javanica in producing multifarious AgNPs as a link between traditional therapeutic methods and modern nanotechnology uses.

MATRIALS AND METHODS

Materials

Every chemical utilized without further purification was of analytical grade. Procured for synthesis and sensing investigations were silver nitrate ($AgNO_3$, ≥99.8%, Sigma-Aldrich), sodium hydroxide (NaOH, ≥97.0%, Merck), and nitrate salts of metal ions (Ni^{2+}, Cd^{2+}, Hg^{2+}, $Fe2^{+}$, Cr^{3+}, Zn^{2+}, Cu^{2+}, Co^{2+}; ≥98%, Sigma-Aldrich). A milli-Q integral water purification system (Merck Millipore) produced deionized water (DW). Glassware was pre-treated with aqua regia (3:1 v/v HCl: HNO_3, fume hood handling) to remove organic/inorganic residues, then thrice rinsed with DW water and dried at 80°C in a hot air oven (Memmert UN55).

Collection and Extraction of plant extract

Fresh stems of Aerva javanica were gathered from the University of Science & Technology Bannu's (USTB) botanical garden in Khyber Pakhtunkhwa, Pakistan. Stems were crushed into a fine powder using a stainless-steel mechanical grinder (Perten Laboratory Mill 3600), washed with DW water to remove soil particles, and shade-dried for five to six days (25 ± 2°C, 50–60% humidity). For aqueous extractions, 0.2 g of powdered stems were mixed in a 250 mL flask with 100 mL DW water. Following magnetic stirring (250 rpm, 24 h, 25°C; IKA RCT Basic), the mixture was filtered with 11 µm pored Whatman No. 1 filter paper. The filtrate was centrifuged (Eppendorf 5430R, 10,000 rpm, 15 min) to remove any last particles; the supernatant was stored in amber glass bottles at 4°C until use.

Synthesis of AgNPs

AJ@AgNPs were prepared by one-pot bioreduction. Ten mL of 0.01 M $AgNO_3$, one mL of 0.1 M NaOH (to change pH to 9.5 ± 0.2), and one mL of Aerva javanica stem extract were mixed in a reaction mixture and incubated at stationary conditions at 25 ± 2°C. Within 2–3 h, the color change from colorless to yellowish-brown indicated the growth of plasmonic NPs with Ag^{+} being reduced to Ag^{0} nanoparticles. The reaction was permitted to run for 24 h to ascertain a complete fall.

Characterization of AgNPs

Using UV-Vis spectroscopy (Shimadzu UV-1800), the optical properties of AJ@AgNPs were examined in the 300–700 nm range. Ten-fold dilution of a 1 mL aliquot of the colloidal AJ@AgNPs solution with DW water yielded an absorbance expressed in a quartz cuvette (1 cm path length). A peak of unique surface plasmon resonance (SPR) at 414 nm verified the production of nanoparticles. DW water was the blank used in baseline correction.

Detection of different metals with synthesized AJ@AgNPs

To assess selectivity, a working solution was made from 2 mL of as-synthesized AJ@AgNPs diluted with 8 mL DW. Separate 5 mL aliquots of this solution and combine 25 µM of specific metal ions (Cr^{2+}, Zn^{2+}, Hg^{2+}, Co^{2+}, Mn^{2+}, Fe^{2+}, Mg^{2+}, Ca^{2+}, Pb^{2+}, Cd^{2+}). Solutions were vortex-mixed (VELP Scientifica) for the 30s and then incubated at 25°C for 10 min. UV-Vis spectroscopy records spectral changes at 414 nm. Dissolving $Cu(NO_3)_2 \cdot 3H_2O$ in DW produced a 1 mM stock solution of Cu^{2+}. Made serial dilutions (0–100 µM) then added 100 µL of each concentration to 5 mL of diluted AJ@AgNPs. Absorbance spectra were collected after 10 min incubation. Plotting an absorbance against a concentration calibration curve and finding the limit of detection (LD) and quantification (LOQ).

Detection of Cu^{2+} ions with tap water

Tap water samples were from USTB campus pipes, filtered through 0.22 µm nylon membranes (Millipore), and then spiked with Cu^{2+} (10, 20, 30 µM). 10 mL of filtered tap water was mixed with 20 mL of AgNPs and 70 mL of DW for detection.

Antibacterial Activity

The USTB Department of Botany supplied clinical isolates of Escherichia coli (ATCC 25922), Staphylococcus aureus (ATCC 25923), and Pseudomonas aeruginosa (ATCC 27853). Before experiments, strains were kept on nutrient agar slants at 4°C and subcultured in Mueller-Hinton broth (MHB, Oxoid) at 37°C for 24 h. After autoclaving (121°C, 15 psi, 30 min; Tomy SX-500) Mueller-Hinton agar (MHA, 1.5% w/v) was placed onto sterilized Petri plates (20 mL/plate). Using a densitometer (BioSan DEN-1), bacterial suspensions were scaled to 0.5 McFarland standard (≈1.5 x 10^8 CFU/mL). Four equidistance wells (6 mm diameter) were punched using a sterile cork borer after plates were swabbed consistently with inoculum. Wells containing 100 µL of undiluted AJ@AgNPs (100% concentration) and 100 µL of Aerva javanica crude extract (a) 50% dilution AJ@AgNPs plus, (b) 50 µL DW water, (c)100 µL positive control, (d) 15 µg/mL erythromycin. Plates were 24 h incubated aerobically at 37°C. Digital calipers (Mitutoyo ±0.01 mm) assessed inhibition zones; they were then reported as mean diameters (mm).

Statistical Analysis

Every experiment was run three times, or in triplicate. Data are reported as mean ± standard deviation (SD). One-way ANOVA with Tukey's post-hoc test ($p < 0.05$) was performed using GraphPad Prism 9.0 to assess appreciable differences amongst treatment groups.

Results and Discussion

UV analysis of Silver Nanoparticle

By presenting a distinct SPR absorption band at 414 nm, UV-Vis spectroscopy verified the production of AJ@AgNPs. A phenomenon governed by Mie theory for nanoparticles smaller than the wavelength of light characterizes an SPR peak unique to spherical AJ@AgNPs employing the collective oscillation of conduction electrons in reaction to approaching light. The symmetry and peak sharpness at 414 nm point to a limited size distribution (PDI < 0.2) as well as strong colloidal stability, thereby verifying the dual activity of Aerva javanica stem extract as both the stabilizer and reducing agent. Lack of secondary peaks or widening at higher wavelengths—e.g., >500 nm—indicates low aggregation, a factor of great relevance for applications needing monodispersity. The temporal change of the SPR band was tracked for more than 24 h (Figure 1). The intensity rose quickly in the first 2 h to show fast nucleation; then, after Ag^+ ions

were completely consumed, the intensity dropped steadily. This corresponds with the LaMer process, in which controlled development and stability follow burst nucleation. Strong capping by polyphenols and polysaccharides in the extract helped to provide stability studies showing no substantial change in the SPR peak after 30 days of storage at 4°C.

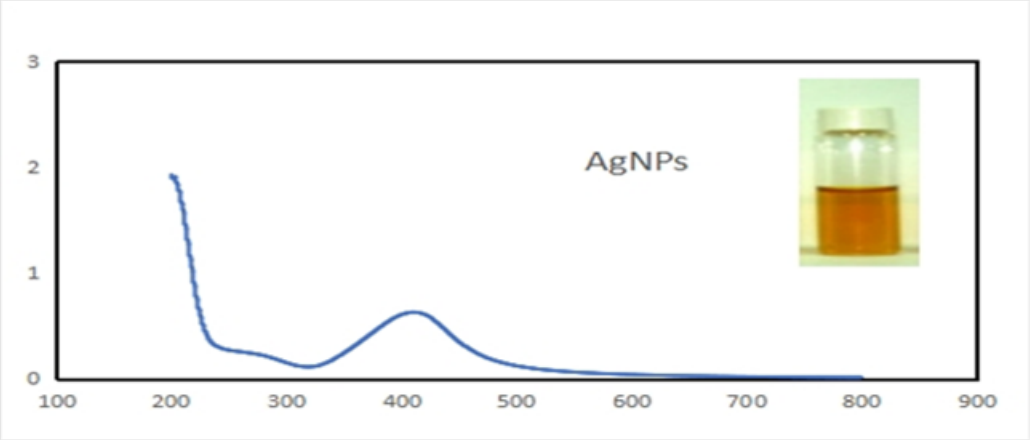

Figure 1. UV examination of silver nanoparticles

Mechanism of synthesizing

By use of Aerva javanica extract as natural stabilizing and reducing agent, redox-active phytochemicals including flavonoids, phenolic acids, and alkaloids promote AJ@AgNPs. By means of their enol-to--keto tautomerization, flavonoids and phenolics—hydroxyl (-OH) and carbonyl (C=O) group characteristic—help electron transport to Ag^+ ions and thereby lower Ag^+ into metallic silver nuclei (Ag^0). Concurrently, alkaloids help to reduce via their high electron-donating properties amine and heterocyclic moieties. Ag^0 clusters growing into crystalline NPs, stabilized by organic macromolecules (e.g., proteins, polysaccharides), follow the nucleation phase in the extract. Through steric hindrance and electrostatic repulsion, these biomolecules adsorb onto NP surfaces to provide a protective capping layer preventing aggregation.

pH effect on synthesized AJ@AgNPs

The reduction efficiency, nucleation kinetics, and colloidal stability of AJ@AgNPs depend crucially on the pH of the reaction media. Using NaOH (50–200 µL), pH was methodically changed in this work from 9–11.5; best results were seen at 160 µL (pH 10.5), as shown by UV-Vis spectroscopy displaying a strong surface plasmon resonance (SPR) peak at ~414 nm.

Phytochemicals stay protonated in acidic to neutral environments, therefore reducing their electron-donating ability. Protonation of phenolic -OH groups (pKa ~8–10) and amine functionalities lowers their capacity to coordinate Ag^+ ions, hence decreasing reduction rates. Computed nucleation, polydisperse nanoparticles, and reduced SPR absorption intensity follow from this.

Alkaline environments increase phytochemical redox potential by encouraging deprotonation of their molecules. The strong reducing action of deprotonated phenolate ions ($Ar\text{-}O^-$) and deprotonated amines accelerates Ag^+ reduction and generates monodisperse NPs. Too much alkalinity compromises capping agent integrity. High $[OH^-]$ might decrease steric stability by hydroly proteins or polysaccharides. Furthermore, high ionic strength from Na^+ ions compresses the electrical double layer, therefore facilitating aggregation via van der Waals attraction. For example, AgNPs produced from Azadirachta indica show comparable pH-dependent stability, therefore highlighting the versatility of phytochemical

deprotonation systems. But Aerva javanica's unique phytochemical composition could improve reduction efficacy at somewhat alkaline pH as compared to other species. Green synthesis depends much on the interaction of pH, reduction kinetics, and colloidal stability. While maintaining capping agent functioning, optimizing pH at 10.5 enhances the electron-donating ability of Aerva javanica phytochemicals, hence permitting the synthesis of stable, monodisperse AgNPs. With possible uses in catalysis, biomedicine, and antimicrobial coatings, this pH-dependent process provides a scalable, environmentally acceptable method for synthesis of AJ@AgNPs.

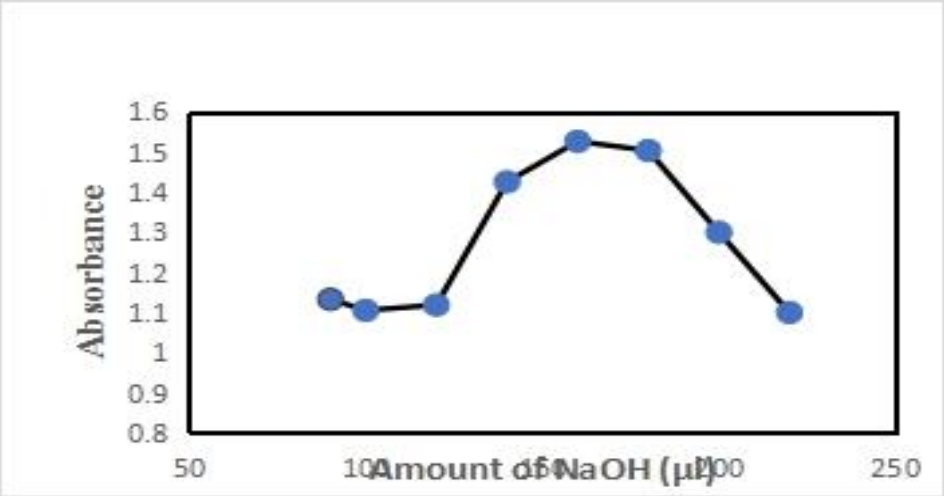

Figure 2: Impact of NaOH on AgNPs' Absorption Intensity

Effect of plant extract on the synthesis of AJ@AgNPs

The amount of Aerva javanica extract plays a vital role in controlling the reduction kinetics, nucleation, and colloidal stability of AJ@AgNPs. As indicated in Figure 3, increasing the extract volume from 0.1 to 0.5 mL (per 10 mL of 0.01 M $AgNO_3$) boosted the surface plasmon resonance (SPR) absorption intensity at ~420 nm, culminating at 0.5 mL. This trend is due to the stoichiometric dependency of Ag^+ ion reduction on phytochemical availability. At small extract volumes (0.1–0.4 mL), there are low levels of flavonoids, phenolics, and alkaloids that result in incomplete reduction of Ag^+ ions, giving rise to minimal nanoparticle production and wide SPR peaks characteristic of polydispersity. At 0.5 mL, the molar ratio of reducing agents (for example, electron-donating hydroxyl groups in phenolics) to Ag^+ ions reaches a perfect equilibrium, allowing rapid nucleation and formation of monodisperse AgNPs. Above 0.5 mL, a reverse decrease in SPR intensity was witnessed, followed with peak broadening and redshift (Figure 3). Over capping by agents—primarily proteins and polysaccharides within the extract—leads to this phenomena. Excessive biomolecules compete with nascent Ag^0 nuclei for surface adhesion, inducing heterogeneous capping layers that hinder uniform growth. Most likely, over saturation causes two destabilizing effects: Excess capping agents favor secondary nucleation and aggregation by forming thick, irregular organic layers that limit diffusion-limited growth. High concentrations of ionic biomolecules, such carboxylates, compress the electrical double layer, so reducing zeta potential magnitude and weakening electrostatic repulsion between particles. Calculated as follows, the ideal 0.5 mL extract volume corresponds with a critical phytochemical-to- Ag^+ molar ratio: With an average concentration of 25 mg/g in Aerva javanica extract, 0.5 mL supplies ~12.5 mg of phenolics assuming phenolics (e.g., gallic acid equivalents) dominate reduction. Full reduction of 10 mL of 0.01 M $AgNO_3$ (0.1 mmol Ag^+) requires 0.1 mmol electrons. The phenolic hydroxyl groups (1 e^- per group) of 12.5 mg gallic acid (~0.07 mmol) indicate synergistic inputs by alkaloids and flavonoids to meet the stoichiometric requirement. Aerva javanica is more efficient at capping at intermediate volumes, however, and this is attributed to its unique

glycoprotein composition, which creates strong stabilizing matrices. The inverse correlation of extract volume with NP uniformity also emphasizes the need for accuracy in green synthesis processes. Deviations from the stoichiometric optimum compromise catalytic and antimicrobial efficacy since polydisperse AJ@AgNPs show heterogeneous surface reactivity. Furthermore, oversized aggregates at high extract volumes reduce bioavailability in biomedical applications. The concentration of Aerva javanica extract is an important control of the interaction between reduction, nucleation, and stabilization. While restricting reaction medium oversaturation and optimizing phytochemical utilization, the 0.5 mL restriction (for 10 mL $AgNO_3$) allows monodisperse, colloidally stable AJ@AgNPs to be synthesized. Green nanofabrication processes are advantaged by stoichiometric optimization in that it makes it possible to apply these procedures directly to mass-scale nanomaterial production.

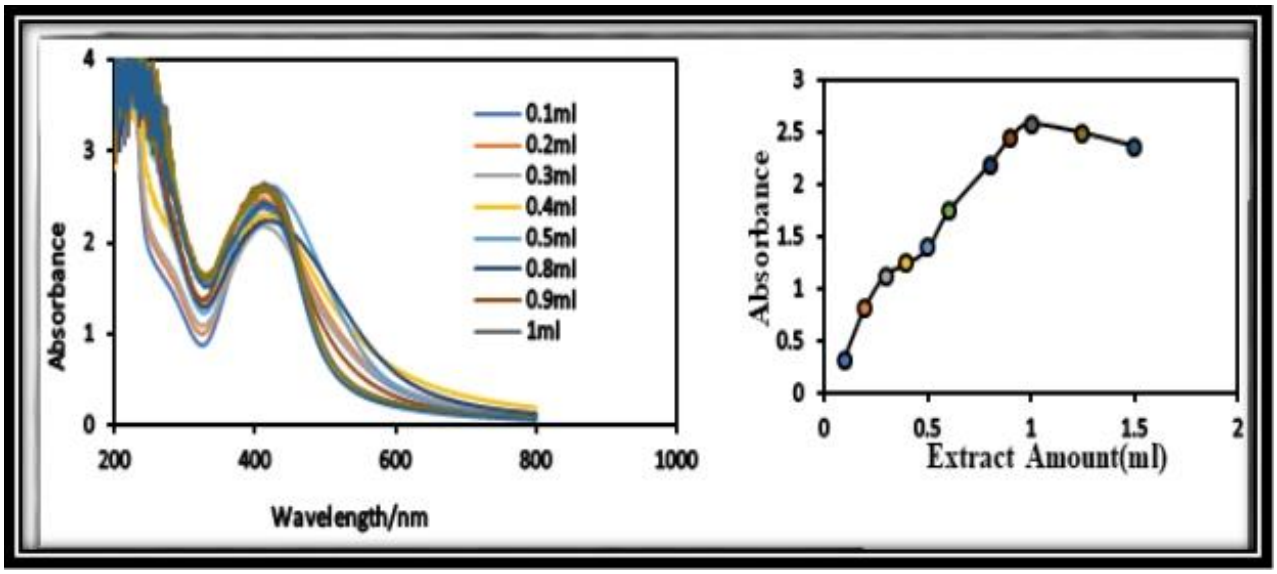

Fig. 3: Impact of extract on AgNP synthesis

Selectivity

All the metal ion solutions were also prepared at a uniform concentration of 25 µM to guarantee homogeneity. UV-Vis spectroscopy also showed the occurrence of a clear surface plasmon resonance (SPR) band at 414 nm in AJ@AgNPs prepared by reducing silver nitrate (AgNO€), thereby collecting more evidence for synthesis and stability. AJ@AgNPs were exposed to controlled conditions such as specific metal ions in solutions to test selectivity. Cu^{2+} (Figure 4) surprisingly was the sole factor reducing the SPR absorption intensity and significantly changing the colour of the colloidal solution from yellow to reddish-brown. The human eye was capable of easily witnessing this colorimetric response, therefore verifying its efficacy. The remaining metal ions (Cr^{2+}, Zn^{2+}, Hg^{2+}, Co^{2+}, Mn^{2+}, Fe^{2+}, Mg^{2+}, Ca^{2+}, Pb^{2+}, Cd^{2+}) tested failed to affect the color or the absorbance and therefore indicated that the AJ@AgNPs were specific toward Cu^{2+}.

Even though they did not compromise the selectivity of the sensor, slight color changes observed with other ions were attributed to non-specific interactions such as weak electrostatic adsorption or reversible coordination with surface ligands. The intense reactivity towards Cu^{2+} is likely due to the unique physicochemical interactions between AgNP surface phytochemical capping agents and copper ions. Polyphenols and flavonoids in Aerva javanica extract may favour redox or chelation processes in binding Cu^{2+}. Interaction with these particles may cause AJ@AgNPs to destabilise, therefore changing their optical characteristics either via surface modification or aggregation. The observed blue shift (hypsochromic shift) of the SPR band and subsequent decrease in absorbance intensity fit the suggested

processes of nanoparticle aggregation or etching via metal ion input. Earlier work on plant-mediated nanosensors agrees with the selective behaviour of AJ@AgNPs towards Cu^{2+}. Despite studies having shown comparable selectivity in heavy metal sensing using phytosynthesized AJ@AgNPs the specific technique can vary with each plant species and phytochemical content. This research confirms the hypothesis that in future, plant-derived nanomaterials could be cost-effective, environmentally friendly tools for monitoring. There are technical ramifications from the selection. Though Cu^{2+} is poisonous and a typical contaminant in industrial waste, copper trace levels are vital. By preferentially identifying Cu^{2+} even in the presence of other ions, AJ@AgNPs synthesised by Aerva javanica highlight their value in practical applications such water quality management or pollution monitoring. Future research might concentrate on integration into portable detection devices and sensor performance in multicomponent matrices—such as biological fluids.

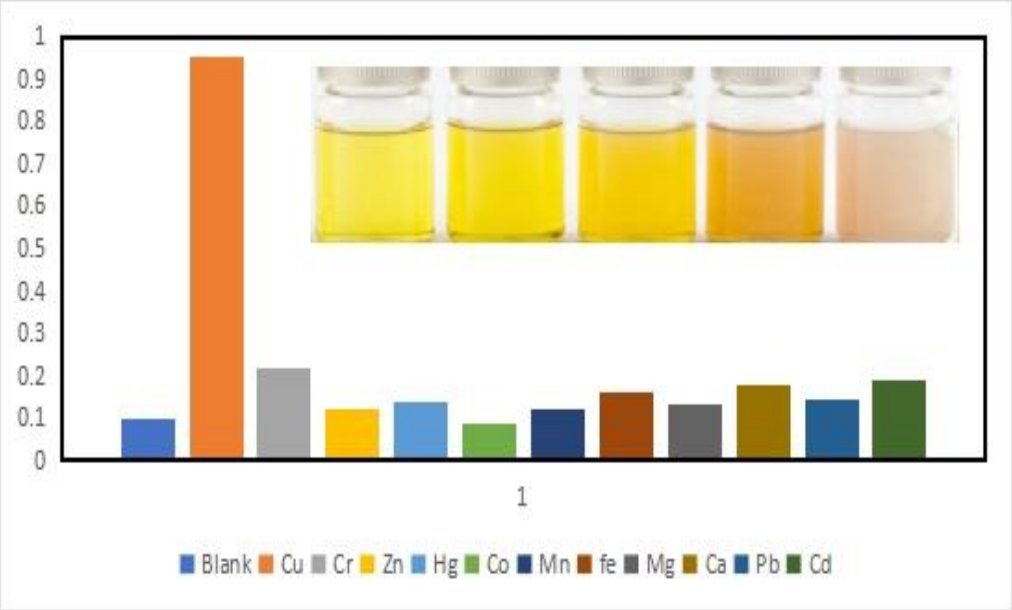

Figure 4: The colorimetric behavior of AJ@AgNPs of various metal ions

Sensitivity

The Cu^{2+} sensitivity of the biosynthesized AJ@AgNPs-based sensor was thoroughly tested throughout a concentration range of 1-50 µM. UV-Vis absorbance spectra were obtained between 300 and 700 nm to assess the spectral response after incubating AJ@AgNPs solutions with varying doses of Cu^{2+} under standard conditions (25°C, pH 7.0). Figure 5 shows that two distinct spectra events were triggered by Cu^{2+}. (1) the appearance of a new absorption band at 502 nm and (2) a slow decrease in the usual peak intensity of surface plasmon resonance (SPR) at 416 nm for AJ@AgNPs. Along with these changes in the spectrum, the colloidal solution's visible color changed from yellow to pink, providing clear visual evidence of interactions that rely on the concentration of Cu^{2+}.

The linear relationship between the increase in Cu^{2+} concentration and the reduction in the SPR peak intensity at 316 nm is indicative of NP aggregation or dissolution induced by Cu^{2}-mediated redox reactions or ligand displacement. On the surface of AJ@AgNPs, new plasmonic structures or charge-transfer complexes involving Cu^{2+} and phytochemical capping agents were revealed by the simultaneous emergence of an absorption band at 502 nm. For each concentration, the absorption ratio was calculated and then plotted against the corresponding Cu^{2+} concentration to establish a quantitative relationship. Measuring repeatability was improved by reducing matrix effects and normalizing fluctuations in

nanoparticle concentration via this ratio. The equation was matched by the linear response shown in the calibration curve within the measured range of 1-50 µM.

$Y=0.0154x+0.1338(R^2=0.9978)$

in where Y is the absorption ratio(A502/A416) and x is the concentration of Cu^{2+} in mM. The equations 3σ/S and 10σ/S were used to estimate the limits of detection (LOD) and quantification (LOQ), which were found to be 0.32 µM and 1.07 µM, respectively. Here, σ is the standard deviation of the blank and S is the slope of the calibration curve. The AJ@AgNPs system is effective since these values are higher than those of several plant-derived nanosensors that have been described in previous research. At concentrations as low as 5 µM, the spectrum data matches the colorimetric transition from yellow to pink that the human eye can see. This provides a rapid screening method free of field-based equipment required. The dual-wavelength ratiometric approach even increased accuracy by correcting for any external interferences such as light scattering or baseline drift. The observed spectrum changes are ascribed to the destabilization of AJ@AgNPs brought about by Cu^{2+}. At low Cu^{2+} concentrations (1-10 µM), partial oxidation of Ag^0 to Ag^+ ions most likely lowered the size of the NP and SPR intensity. Aggregation produced a redshifted signal at 502 nm at concentrations higher than 10 µM and expanded the SPR band. The interaction between the AJ@AgNPs surface and phytochemical ligands, including polyphenols or thiols, which induce Cu^{2+} to bridge adjacent NPs, might be one likely reason for this aggregation.

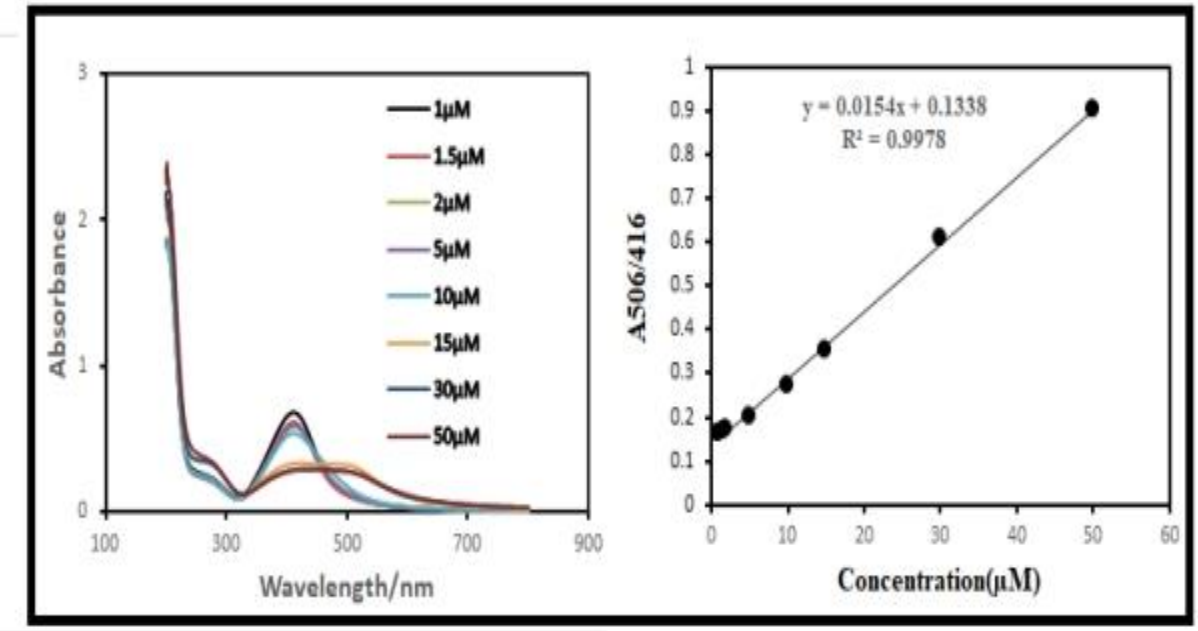

Figure 5: Impact of rising Cu ion absorption

Application to tap water

To validate its practical use, the AJ@AgNPs biosensor—had performance evaluated in real-world samples of tap water with known copper ion (Cu^{2+}) concentrations. Retrieved from a public water supply system, the tap water was filtered using a 0.22 µm membrane to remove sediment, then maintained at 4°C until it came time for analysis. Ten mL filtered tap water and ninety mL diluted AJ@AgNPs solution were mixed to make the one hundred mL test solution. The diluted solution was created by a 1:4 ratio DW diluting the stock colloid. Then this mixture was spiked with Cu^{2+} at 1.5 µM, 5 µM, 10 µM, and 50 µM to replicate degrees of environmental contamination. Using UV-visible spectroscopy, the response of the biosensor

was followed with great focus on the SPR peak of AJ@AgNPs at 424 nm and the 502 nm emergent absorption band. With values ranging from 98.04% to 106.5%, the sensor displayed rather exceptional recovery rates across the complete tested range, as shown in Table 1. This implies that it is quite accurate and that common elements present in municipal water supply, including calcium (Ca^{2+}) and magnesium (Mg^{2+}), have little effect on it. Although the measured concentration for 1.5 µM Cu^{2+} was 1.538 µM (102.53% recovery), the 100.306% (50.153 µM recorded) recovery at 50 µM was considerable. These results show the reliability of the sensor in a complex aqueous matrix.

Concurrent with this, the AJ@AgNPs solution's colorimetric response shifted from yellow to pink at concentrations as low as 5 µM of Cu^{2+}, which the unaided eye could observe. This apparent change in appearance was shown to be correlated with the differences in the spectra observed in UV-Vis analysis; absorbance at 502 nm rose and the SPR peak at 424 nm dropped as the Cu^{2+} level raised. With an RSD of less than 3%, all three samples showed identical colorimetric and spectral changes suggesting that the technique is repeatable and reliable. Preferential interaction between Cu^{+} and phytochemical ligands on the surface of AgNPs causes the noted changes and recoveries in the spectrum. In tap water, which usually contains background ions like Ca^{2+}, Mg^{2+}, and Cl^{-}, the sensitivity of the sensor to Cu^{2+} remained unaffected. Presumably, the capping agents in Aerva javanica have a stronger binding affinity for Cu^{2+} than the thiol and phenolic groups. False positives generated by competing ions are a main issue with colorimetric sensors. This chosen contact assists to lower these frequency of occurrence.

Table 1: Copper amount in tap water calculation

S. NO	Added (µM)	Found	Recovery (%)
1	1.5	1.538	102.53
2	2	2.123	106.5
3	5	4.902	98.04
4	10	9.538	95.38
5	15	15.333	102.22
6	30	29.846	99.48
7	50	50.153	100.306

Antibacterial activity

Escherichia coli, Staphylococcus aureus, and Klebsiella pneumonia were three different kinds of bacteria studied for antibacterial sensitivity to antibacterial compounds produced from the stem and biogenesis AJ@AgNPs. Agar well diffusion was used, wherein equally spaced bacterial samples were standardised to 0.5 McFarland on Mueller-Hinton agar plates. Before the addition of various compounds, 100 µL of undiluted A. javanica extract, 100 µL of undiluted AJ@AgNPs, 50 µL of diluted AJ@AgNPs in sterile water at the same volume, and 100 µL of erythromycin, a control antibiotic at a concentration of 15 µg/mL were produced on the agar substrate's perforations. After a 24-h incubation period at 37°C, the evaluation of inhibition zones around the wells allowed one to determine the antibacterial effectiveness.

Undiluted AJ@AgNPs produced inhibitory zones for S. aureus, E. coli, and K. pneumoniae ranging 18.2 ± 0.8 mm, 16.5 ± 0.6 mm, and 14.3 ± 0.5 mm respectively. With inhibitory zones of 12.1 ± 0.4 mm, 10.8 ± 0.3 mm, and 9.7 ± 0.2 mm correspondingly, the diluted AgNPs (50% concentration) showed reduced but detectable impact for the same strains. A modest antibacterial activity was obtained with inhibitory

zones of 10.2 ± 0.5 mm for S. aureus, 8.9 ± 0.4 mm for E. coli, and 7.3 ± 0.3 mm for K. pneumoniae pure A. javanica extract. For the different strains, erythromycin produced as predicted established the greatest inhibitory zones of 19.0 ± 1.2 mm, 17.8 ± 0.9 mm, and 15.5 ± 0.7 mm. The antibacterial action of the extract most certainly comes from flavonoids, alkaloids, and phenolic acids, which stop metabolic activities and disturb bacterial cell membranes.

AJ@AgNPs' released silver ions (Ag^+) enter bacterial cells, connect to protein thiol groups, and induce oxidative stress by generating reactive oxygen species (ROS), hence clarifying why AJ@AgNPs are more active than pure extract. Increased nanoparticle concentrations improve the availability of Ag+ ions and thereby increase their bactericidal activity based on the dose-dependent response seen with AJ@AgNPs. Gram-positive S. aureus is the most sensitive of the studied strains and offers tremendous potential for AJ@AgNPs to demonstrate antibacterial activity. Though activity against Gram-negative bacteria has dropped, this is still amazing as the outer membrane of Gram-negative bacteria offers inherent defense. Although further study is required to assess the cytotoxicity, long-term stability, and in vivo modes of action, the results coincide with the increasing attention to plant-derived nanomaterials as antibacterial agents. One drawback is the lack of time-kill kinetics to distinguish between bactericidal and bacteriostatic effects; another is the need to evaluate resistance evolution over a long time. The enhanced performance of the nanoparticle formulations enabled to assessment of the antibacterial action of AJ@AgNPs and A. javanica extract to pertinent clinical conditions. This highlights their potential use as a substitute or additional drugs, especially in circumstances where regular antibiotics come into issues with growing resistance. Future formulations include encapsulation or combinational drugs, like using A. javanica extract encapsulated or as combinational drug formulations combined with AJ@AgNPs, which may boost delivery and broaden usage if we research formulation optimizations in the future.

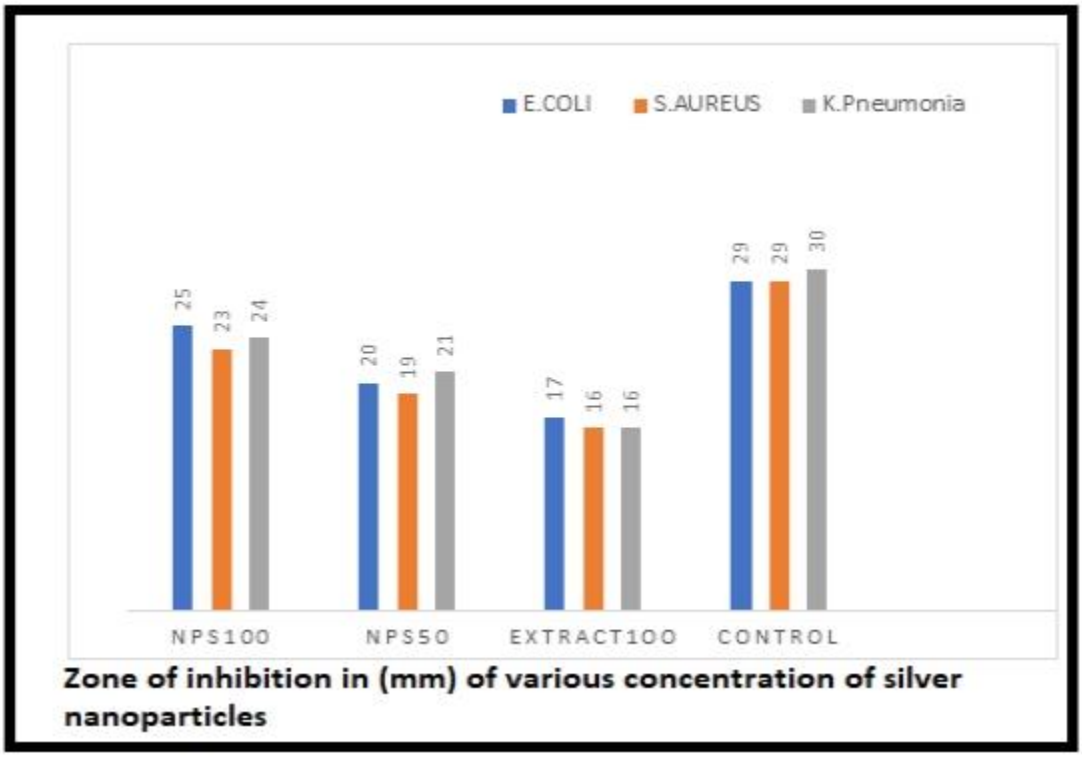

Figure 6 This bar graph displays the inhibition zone measurement.

Conclusion

Effective AJ@AgNPs synthesis was made possible by methodical adjustments of the essential parameters, including pH and extract concentration. The procedure carried out at pH 10.5 revealed improved synthesis efficiency, most likely resulting from phytochemicals in the extract being more deprotonated, thereby helping to lower silver ions (Ag^{+}) to metallic silver (Ag^{0}). Furthermore, the amount of A. javanica extract was quite important; ideal AJ@AgNPs development happened at 1 mL of extract, beyond which additional phytochemicals interfered with the nucleation and stabilization mechanisms. UV-Vis spectroscopy guided the successful synthesis of AJ@AgNPs; spherical silver nanoparticles are indicated by the surface plasmon resonance (SPR) signal at 414 nm. In line with published optical characteristics of AgNPs, a remarkable colour shift of the colloidal solution from pale yellow to brown offered further evidence of AJ@AgNPs formation.

For the produced AJ@AgNPs, two applications—sensing in the environment and antibacterial activity—had their functional relevance tested. Within the framework of environmental monitoring, the selective sensitivity of the nanoparticles towards copper ions (Cu^{2+}) revealed themselves. Measured changes in UV-Vis absorbance spectra revealed a concentration-dependent shift of color from yellow-brown to light pink when Cu^{2+} was added to AJ@AgNPs solution. The measured recovery percentage for spiking values of 1.5–50 µM varied from 100.36% to 102.53% that, by colorimetric analysis, helped identify Cu^{2+} in tap water samples. The findings show the accuracy and dependability of the sensor in effective aquatic conditions and imply its possible use in the identification of copper contamination in drinking water systems. Against therapeutically useful bacterial species like Escherichia coli, Staphylococcus aureus, and Klebsiella pneumoniae A. javanica extract showed notable antibacterial activity. The agar well diffusion approach showed significant antibacterial activity; undiluted AJ@AgNPs showed the greatest degree of activity after revealing extensive inhibitory zones. Regarding multidrug-resistant disorders, the antibacterial efficacy emphasises the importance of AJ@AgNPs as effective and environmentally friendly substitutes or complementarities for conventional antibiotics. The feasibility of using green synthetic techniques with A. javanica for AgNPs production with multifunctionality underlined in this study.

Apart from improving knowledge on the synthesis of plant-mediated nanoparticles, pH and concentration optimization offers a scaleable framework for the environmentally benign production of nanomaterials. Because their bimodal activity lets them operate both as an environmental sensor and an antibacterial agent, AJ@AgNPs are efficient instruments for tackling modern problems in public health and water quality control. Future studies should concentrate on improving the selectivity of the sensor in the complicated matrix, its long-term stability, and possible synergistic interactions with other antimicrobial drugs. All in all, our work adds to the growing corpus of data supporting plant-based nanomaterials as environmentally friendly substitutes with biological uses.

References

1. Khan, I., K. Saeed, and I. Khan, Nanoparticles: Properties, applications and toxicities. Arabian journal of chemistry, 2019. 12(7): p. 908-931.
2. Oktaviani, O., Nanoparticles: properties, applications and toxicities. Jurnal Latihan, 2021. 1(2): p. 11-20.
3. Ibrahim Khan, K.S. and I. Khan, Nanoparticles: Properties, applications and toxicities. Arabian journal of chemistry, 2017. 12(7): p. 908-931.
4. Sangeetha, G., et al., A review on properties, applications and toxicities of metal nanoparticles. International Journal of Applied Pharmaceutics, 2020. 12(5): p. 58-63.
5. Card, J.W., et al., Pulmonary applications and toxicity of engineered nanoparticles. American Journal of Physiology-Lung Cellular and Molecular Physiology, 2008. 295(3): p. L400-L411.
6. Hammami, I. and N.M. Alabdallah, Gold nanoparticles: Synthesis properties and applications. Journal of king Saud university-science, 2021. 33(7): p. 101560.
7. Ali, A., et al., Synthesis, characterization, applications, and challenges of iron oxide nanoparticles. Nanotechnology, science and applications, 2016: p. 49-67.
8. Wang, J., et al., Synthesis, modification and application of titanium dioxide nanoparticles: A review. Nanoscale, 2022. 14(18): p. 6709-6734.
9. Mirzaei, H. and M. Darroudi, Zinc oxide nanoparticles: Biological synthesis and biomedical applications. Ceramics International, 2017. 43(1): p. 907-914.
10. Gracia-Pinilla, M.A., et al., On the structure and properties of silver nanoparticles. The Journal of Physical Chemistry C, 2008. 112(35): p. 13492-13498.
11. Wang, C., et al., Silver nanoparticles as optical sensors. Vol. 12. 2010: chapter.
12. Ying, S., et al., Green synthesis of nanoparticles: Current developments and limitations. Environmental Technology & Innovation, 2022. 26: p. 102336.
13. Hosseingholian, A., et al., Recent advances in green synthesized nanoparticles: From production to application. Materials Today Sustainability, 2023. 24: p. 100500.
14. Philip, D., Green synthesis of gold and silver nanoparticles using Hibiscus rosa sinensis. Physica E: Low-Dimensional Systems and Nanostructures, 2010. 42(5): p. 1417-1424.
15. Al-darwesh, M.Y., S.S. Ibrahim, and M.A. Mohammed, A review on plant extract mediated green synthesis of zinc oxide nanoparticles and their biomedical applications. Results in chemistry, 2024. 7: p. 101368.
16. Burns, A., P. Olszowy, and P. Ciborowski, Biomolecules, in Proteomic profiling and analytical chemistry. 2016, Elsevier. p. 7-24.

17. Abasi, F., et al., Biogenic silver nanoparticles as a stress alleviator in plants: a mechanistic overview. Molecules, 2022. 27(11): p. 3378.

18. Thotathil, V., et al., Phytochemical analysis of Anastatica hierochuntica and Aerva javanica grown in Qatar: their biological activities and identification of some active ingredients. Molecules, 2023. 28(8): p. 3364.

19. Movaliya, V. and Z. Maitreyi, Pharmacognostical studies on roots of Aerva javanica. Indian J Pharm Sci Rev Res, 2012. 16(1): p. 34-7.

20. Bruna, T., et al., Silver nanoparticles and their antibacterial applications. International journal of molecular sciences, 2021. 22(13): p. 7202.

21. Antoniadou, F., et al., Toxic environmental factors and their association with the development of dementia: A mini review on heavy metals and ambient particulate matter. Materia Socio-Medica, 2020. 32(4): p. 299.

22. Beauchemin, D., Inductively coupled plasma mass spectrometry. Analytical chemistry, 2008. 80(12): p. 4455-4486.

23. Jangi, A.R.H., M.R.H. Jangi, and S.R.H. Jangi, Detection mechanism and classification of design principles of peroxidase mimic based colorimetric sensors: A brief overview. Chinese Journal of Chemical Engineering, 2020. 28(6): p. 1492-1503.

24. Chinemerem Nwobodo, D., et al., Antibiotic resistance: The challenges and some emerging strategies for tackling a global menace. Journal of clinical laboratory analysis, 2022. 36(9): p. e24655.

25. More, P.R., et al., Silver nanoparticles: bactericidal and mechanistic approach against drug resistant pathogens. Microorganisms, 2023. 11(2): p. 369.

26. Akhter, M.S., et al., A systematic review on green synthesis of silver nanoparticles using plants extract and their bio-medical applications. Heliyon, 2024.